ADVANCED MATERIALS
www.advmat.de

www.MaterialsViews.com

Multi Ball-In-Ball Hybrid Metal Oxides

*Won Cho, Yun Hee Lee, Hee Jung Lee, and Moonhyun Oh**

Many examples of micro- and nanoscale particles made from atomic or molecular building blocks are known, with these systems having been extensively explored due to their useful properties.[1–6] Currently, efforts are ongoing to manipulate the composition, as well as its size and morphology, of particles as part of systematic attempts to alter their chemical and physical properties. Within this context, chemical transformation has emerged a useful method for tuning the composition.[7,8] Metal oxide materials have received a great deal of attention as a result of their functional properties that have made them of use in a wide range of fields including magnetics,[9] electronics,[10] optics,[11] catalysis,[12] and medical diagnostics.[13] ZnO and Co_3O_4, in particular, are attractive materials because they are a nonexpensive and nontoxic photoluminescent semiconductor and a magnetic *p*-type semiconductor, respectively. And they have many interesting applications in sensor, catalyst, electronic device, and solar cell.[10–12] Some hybrid metal oxide materials containing more than two metal composites within a particle have been described; these display modified properties and have been proposed as candidates for multifunctional materials;[14,15] however, there is no general preparation method for hybrid metal oxide materials with tunable chemical compositions. Here we formulate a methodology that involves straightforward chemical transformation and continuous thermal treatment of the colloidal coordination polymer particles (CPPs) and show that it allows for the synthesis of composition-tunable multi ball-in-ball hybrid metal oxide particles through the cation exchange reaction. The work described here thus provides a way to access a variety of multicompositional hybrid metal oxides, something that should facilitate their eventual use in practical applications.

Infinite coordination polymers in which metal ions or metal clusters act as nodes to connect molecular building blocks consisting of organic or organometallic complexes have received many attention because of their useful applications such as gas storage, catalysis, optics, and separation.[16] Recently, the novel strategies for the synthesis of micro- and nano-sized particles made from infinite coordination polymers, namely coordination polymer particles (CPPs), have been proposed and demonstrated.[2,8,17–20] Taking advantage of the unique reactivity and thermal behavior of CPPs, a number of spherical multi ball-in-ball hybrid metal oxides with tunable compositions have been logically formulated and prepared using the following straightforward processes; I) CPP preparation using a precipitation method, II) cation exchange reaction for composition transformation of CPPs, and III) a final calcination processing of pre-prepared CPPs that engenders decomposition of the CPPs and formation of metal oxides (**Scheme 1**). In general, the initial spherical CPPs, namely M-MSB-M (**2**, M = Zn^{2+} or Co^{2+}, MSB = metallo Schiff base, see structure in Scheme 1) have been constructed from a Schiff base (**1**) and transition metal ions. Subsequently, these mono-metallic M-MSB-M (**2**) particles were mixed with a secondary metal ion (e.g., M' = Cu^{2+}, Co^{2+}, or Ni^{2+}) to effect the cation exchange and produce the requisite bimetallic CPPs, M'-MSB-M (**3**). Thermal treatment of **2** and **3** at 450 ~ 550 °C then results in the formation of multi ball-in-ball metal oxides (**4**) and multi ball-in-ball hybrid metal oxides (**5**), respectively, with compositions of M'_vO_w/M_xO_y (M and M' = Zn (**4a**); M and M' = Co (**4b**); M = Zn, M' = Cu (**5a**); M = Zn, M' = Co (**5b**); M = Co, M' = Cu (**5c**); M = Co, M' = Ni (**5d**)).

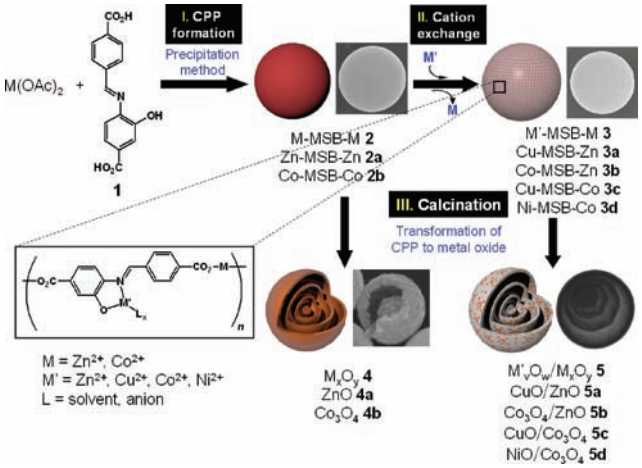

Scheme 1. Preparation of multi ball-in-ball hybrid metal oxides.

The initial spherical Zn-MSB-Zn (**2a**) particles with an average diameter of 1.93 ± 0.43 μm (**Figure 1**a), were synthesized from a solution containing both zinc acetate and the Schiff base (**1**), using a precipitation method.[2,8] The formation of spherical particles, especially for the amorphous materials, is usually elucidated by the tendency to minimize the surface tension during particle formation.[21] The compositions and general properties of the resulting CPPs were determined using conventional methods, including field-emission scanning electron microscopy (FE-SEM), optical microscopy (OM), fluorescence microscopy (FM), infrared (IR) spectroscopy, energy dispersive X-ray (EDX) spectroscopy, inductively coupled plasma (ICP) analysis, emission spectroscopy, powder X-ray diffraction (PXRD) spectroscopy, and thermogravimetric analysis (TGA) (see Figure 1 and Supporting Information). As would

W. Cho, Y. H. Lee, H. J. Lee, Prof. M. Oh
Department of Chemistry
Yonsei University
134 Shinchon-dong, Seodaemun-gu, Seoul 120–749, Korea
E-mail: moh@yonsei.ac.kr

DOI: 10.1002/adma.201004493

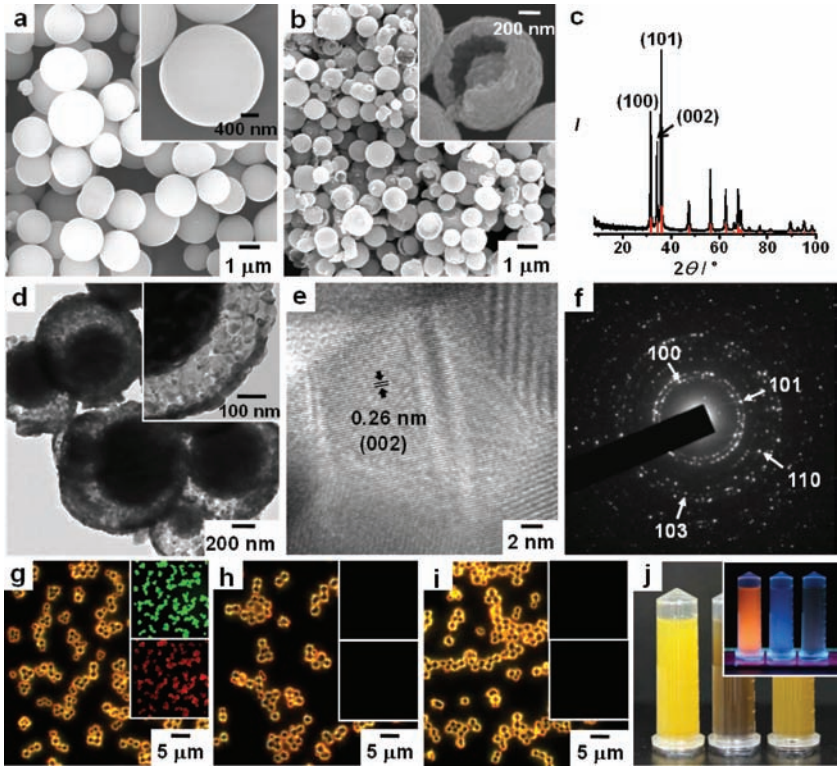

Figure 1. a) SEM images of Zn-MSB-Zn (**2a**). b) SEM images and c) PXRD spectrum of ball-in-ball ZnO (**4a**). Red lines are the reported values of the hexagonal wurtzite phase of pure ZnO (JCPDS Card No. 36–1451). d) TEM images, e) HRTEM image, and f) SAED pattern of **4a**. OM and FM (insets) images measured before and after the cation exchange reactions. Images were obtained from samples of g) Zn-MSB-Zn (**2a**), h) Cu-MSB-Zn (**3a**), and i) Co-MSB-Zn (**3b**). j) Photographs of a series of CPPs (left to right: **2a**, **3a**, and **3b**) without and with (inset) UV irradiation.

be expected given the fluorescent nature of the Zn-metallated Schiff base (Zn-MSB) building blocks,[2,19] Zn-MSB-Zn (**2a**) particles proved fluorescent.

Zinc oxide particles (**4a**) were then prepared by the calcination of Zn-MSB-Zn at 550 °C for 60 min using a conventional furnace. During the calcination process, Zn-MSB-Zn were decomposed to zinc oxide, as confirmed by chemical composition change, PXRD spectra, lattice fringe, and selected area electron diffraction (SAED) patterns. The chemical composition of the resulting zinc oxide was determined using EDX spectroscopy, in which only zinc and oxygen atoms were observed (Figure S3). In contrast, the EDX spectrum of the initial Zn-MSB-Zn showed a strong carbon atom peak due to the presence of the organic building blocks. The PXRD spectra taken before and after the thermal treatment revealed the formation of a hexagonal wurtzite structured ZnO, as inferred from observed change in the spectrum from a featureless diffraction pattern of amorphous Zn-MSB-Zn to a clearly shaped spectrum wherein all of the observed peaks matched exactly with the values reported for the hexagonal wurtzite structure[22] (Figure 1c). As shown in the high-resolution transmission electron microscopy (HRTEM) image, the lattice fringe image revealed a calculated planar space of 0.26 nm in the (002) plane of the hexagonal wurtzite ZnO (Figure 1e). The SAED pattern (Figure 1f) of **4a**, in addition, exhibited the hexagonal wurtzite phase of ZnO.

The SEM images revealed that the resulting ZnO particles maintained original spherical shape; however, the size was reduced by approximately 40% relative to the original Zn-MSB-Zn particles, due to the removal of the organic building blocks during the calcination process. The transformation of CPPs into metal oxides through calcination process is typically accompanied by maintaining the original morphology of the CPPs.[19a,23] As shown in Figure 1d,e, Zn-MSB-Zn was transformed into a polycrystalline ZnO particle[24] comprised of ca. 35 nm sized ZnO nanocrystals (also see Figure S12). Furthermore, a unique ball-in-ball structure was verified by the SEM and TEM images (Figure 1b,d). This ball-in-ball structures can be utilized in many useful applications, such as catalysts, drug carriers, sensor systems, and nano-reactors, as would be expected in the hollow particles.[25] For example, the incorporation of doxorubicin (DOX, anticancer agent) into ball-in-ball particles can be achieved by mixing the poly(ethylene glycol) coated particles with DOX.[25d,e] Insights into the formation of these new and unique ball-in-ball structured particles were obtained by considering the CPP's thermal decomposition process. The CPP most likely transforms into metal oxide in a slow and progressive way (see the TGA curve in Figure S4) starting from the outside of the CPP, a process which induces a stepwise formation of ZnO from the outermost part of the particle. Following the initial formation of the first zinc oxide layer on the exterior of the particle, the internal coordination polymer component shrinks again; this then continues on as the process of decomposition into the metal oxide runs its course. This stepwise formation of metal oxide layers will result in a ball-in-ball structure.

In addition to preparing ZnO-derived ball-in-ball structures, we found that hybrid metal oxide structures could be obtained by modifying the composition of the initial CPPs. These composition transformations were typically effected by preparing a mixture of Zn-MSB-Zn particles and Cu^{2+} (or Co^{2+}) in methanol and letting it stand under ambient conditions. This led to a change in the composition of the CPPs, a transformation that could be monitored easily by OM and FM (Figure 1g–i). Within one hour, most of the fluorescent Zn-MSB-Zn particles were converted into non-fluorescent Cu-MSB-Zn, and the reaction was terminated after five hours. The loss of fluorescence indicates an exchange of Cu^{2+} for the Zn^{2+} ions coordinated to the bidentate Schiff base moieties within the initial CPP.[8] Both Zn-MSB building blocks and Zn-MSB-Zn particles are fluorescent; however, the product resulting from cation exchange, Cu-MSB, is not fluorescent.[2,8] The ion exchange process could be also followed by the naked eye, as evidenced by a color change from yellow (Zn-MSB-Zn) to brown (Cu-MSB-Zn, Figure 1j). Further evidence for ion exchange came from the

EDX spectrum of the resulting Cu-MSB-Zn particles (**3a**); after the cation exchange this showed the expected Cu signal, in addition to that of Zn (Figure S3). Finally, ICP analyses[26] were consistent with a change in the number of metal ions within the CPP particles, from roughly two to one Zn^{2+} and from zero to one Cu^{2+} per subunit as the between Zn-MSB-Zn and Cu-MSB-Zn was effected on the whole particles.

We also prepared Co-MSB-Zn particles (**3b**) using a similar method. However, in contrast to what was seen under the conditions of Cu^{2+} exchange, an excess Co^{2+} had to be employed in order to obtain a significant degree of conversion (Figure 1i). The optical features,[27] the EDX spectrum, and ICP analysis[26] of the reaction products revealed the formation of the Co-MSB-Zn particles (see Supporting Information). A comparison of the SEM images of the initial Zn-MSB-Zn and cation exchanged M'-MSB-Zn particles provided evidence that the size and shape of the particles were preserved after the reaction (Figure S2).

Finally, the hybrid metal oxides were prepared by a calcination of M'-MSB-Zn at 550 °C for 60 min using a conventional furnace. The chemical compositions of the resulting hybrid metal oxides were determined using EDX spectroscopy, in which only zinc, oxygen and the exchanged metal (copper for **5a** or cobalt for **5b**) atoms were observed (Figure S3). The PXRD spectra of the resulting particles revealed that they have both ZnO and CuO (or Co_3O_4) structures (Figure S7 and **Figure 2**). All of the observed peaks matched exactly with the reported values of the hexagonal wurtzite structure of ZnO and the monoclinic structure[28] of CuO (or the spinel structure[12] of Co_3O_4). The elemental mapping data[29] of **5a** and **5b** provides support for the conclusion that the hybrid metal oxides contain both Zn and Cu or both Zn and Co, respectively (Figure S7 and Fit2f). The resulting hybrid metal oxides, **5a** and **5b**, were composed of numerous ZnO and CuO (or Co_3O_4) nanocrystals.

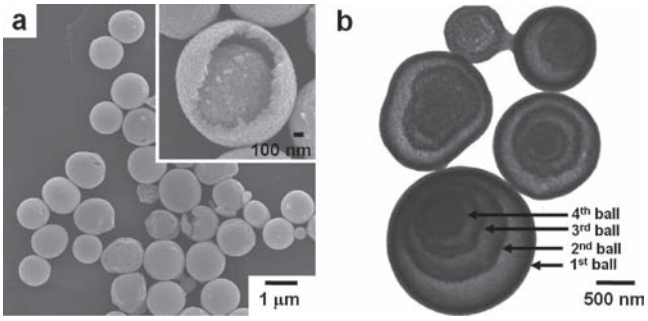

Figure 3. a) SEM and b) TEM images of NiO/Co_3O_4 (**5d**). Images clearly show a multi ball-in-ball structure for up to four continuous balls.

As shown in the HRTEM images (Figure S7 and Figure 2d), analysis of the lattice fringe images is consistent with a calculated planar space of 0.26 nm in the (002) plane of the hexagonal wurtzite ZnO, 0.23 nm in the (111) plane of the monoclinic structure CuO, and 0.45 nm in the (111) plane of the spinel structure Co_3O_4. The results of SAED patterns of **5a** and **5b** coincided with the observations from the lattice fringe and the PXRD results. In order to analyze the internal particle, the particles were embedded in an epoxy matrix and cut into thin sections with a microtome. Interestingly, the SEM images of the sectioned particles by microtome clearly reveal the formation of a multi ball-in-ball structure (Figure 2b). In addition, support for this multi ball-in-ball structure came from TEM images (Figure 2c). These analyses revealed ball-in-ball particles consisting of up to four continuous balls in the case of Co_3O_4/ZnO **5b** (Figure 2b,c and Figure S8), Co_3O_4 **4b** (Figure S9), and NiO/Co_3O_4 **5d** (**Figure 3**).

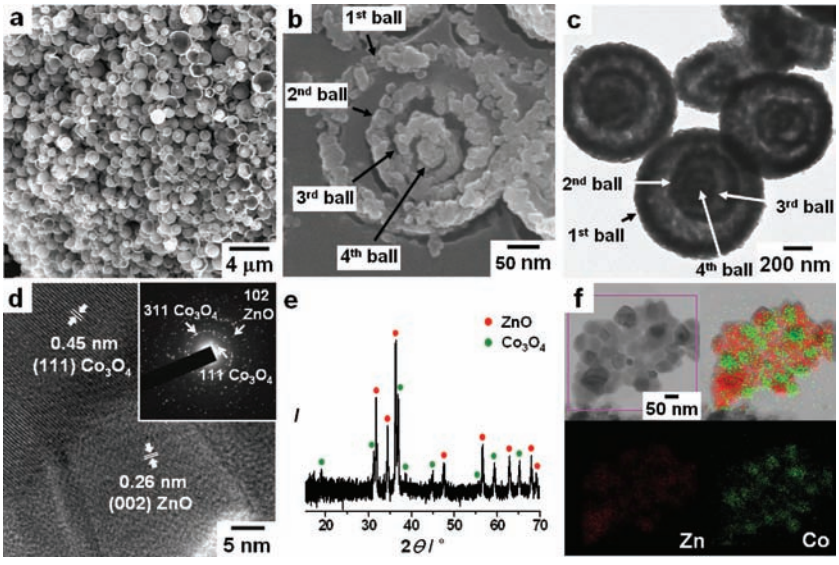

Figure 2. a) SEM image of Co_3O_4/ZnO (**5b**). b) SEM image of the sectioned particles obtained by microtome. c) TEM and d) HRTEM images of **5b**. The lattice fringe image shows the coexistence of ZnO and Co_3O_4. Inset in (d) is SAED pattern. e) PXRD spectrum of **5b**. Red and green dots are the reported values of the hexagonal wurtzite phase of pure ZnO (JCPDS Card No. 36–1451) and the spinel structure of pure Co_3O_4 (JCPDS Card No. 42–1467), respectively. f) Elemental mapping data for **5b**. STEM image of the fraction of **5b** (top left), overlapping image of Zn and Co mapping (top right), Zn mapping image (bottom left), and Co mapping image (bottom right).

To verify the generality of this new approach for the preparation of a series of hybrid metal oxides, an analogue of the initial spherical CPP, Co-MSB-Co (**2b**), was prepared using $Co(OAc)_2$ instead of $Zn(OAc)_2$ as the metal cation source (see Supporting Information). These precursors provided multi ball-in-ball Co_3O_4 (**4b**), when subject to a calcination treatment similar to that described above (Figure S9). Further, the cation exchange reactions involving the Co-MSB-Co particles and Cu^{2+} or Ni^{2+} resulted in the formation of compositions assigned to be Cu-MSB-Co (**3c**) or Ni-MSB-Co (**3d**), respectively, as confirmed by EDX spectral and ICP analyses[30] (see Supporting Information). The calcination of **3c** and **3d** at 450 °C for 60 min eventually produced hybrid metal oxides (Figure 3 and Figure S10,11). The EDX spectra of these products revealed the presence of only cobalt, oxygen and the exchanged metal (copper for **5c** or nickel for **5d**). The PXRD spectra of these hybrid metal oxides further confirmed that they have both

Co_3O_4 and CuO (or NiO) structures. All of the observed peaks were identical to the reported values of the spinel structure of Co_3O_4 and the monoclinic structure of CuO (or the NaCl structure[31] of NiO). The size and structure of **5c** and **5d** were characterized by SEM and TEM, in which multi ball-in-ball particles for up to four continuous balls were clearly seen. In last, the magnetic property measurements of the present hybrid metal oxides were analyzed; this revealed properties that were strongly dependent on their chemical compositions, meaning that this property could be tailored through synthesis (Figure S13).

In conclusion, we have demonstrated that a strategy for the synthesis of composition-tunable hybrid metal oxide particles with a unique multi ball-in-ball structure consisting of up to four continuous balls by taking advantage of the unique reactivity and thermal behavior of CPPs. Since CPPs of the general form M'-MSB-M can be prepared using a wide range of metal species, M and M'; therefore, this methodology will allow for a new, general strategy for preparing many new composition-customized hybrid metal oxides. As such, it is expected to open up a route towards materials with novel properties and that will see use in a variety of applications.

Supporting Information

Supporting Information is available from the Wiley Online Library or from the author.

Acknowledgements

This work was supported by a grant (no. KRF-2008–313-C00439), the Mid-career Researcher Program (no. 2009–0079545), and the WCU program (no. R32–2008-000–10217-0) through NRF grant funded by the MEST.

Received: December 7, 2010
Revised: January 13, 2011
Published online: February 23, 2011

[1] M. Bruchez Jr., M. Moronne, P. Gin, S. Weiss, A. P. Alivisatos, *Science* **1998**, *281*, 2013.
[2] M. Oh, C. A. Mirkin, *Nature* **2005**, *438*, 651.
[3] H. Zeng, J. Li, J. P. Liu, Z. L. Wang, S. Sun, *Nature* **2002**, *420*, 395.
[4] C. A. Witham, W. Huang, C.-K. Tsung, J. N. Kuhn, G. A. Somorjai, F. D. Toste, *Nat. Chem.* **2010**, *2*, 36.
[5] Y. C. Cao, R. Jin, C. A. Mirkin, *Science* **2002**, *297*, 1536.
[6] M. J. MacLachlan, N. Coombs, G. A. Ozin, *Nature* **1999**, *397*, 681.
[7] D. H. Son, S. M. Hughes, Y. Yin, A. P. Alivisatos, *Science* **2004**, *306*, 1009.
[8] M. Oh, C. A. Mirkin, *Angew. Chem. Int. Ed.* **2006**, *45*, 5492.
[9] I. S. Lee, N. Lee, J. Park, B. H. Kim, Y.-W. Yi, T. Kim, T. K. Kim, I. H. Lee, S. R. Paik, T. Hyeon, *J. Am. Chem. Soc.* **2006**, *128*, 10658.
[10] K. T. Nam, D.-W. Kim, P. J. Yoo, C.-Y. Chiang, N. Meethong, P. T. Hammond, Y.-M. Chiang, A. M. Belcher, *Science* **2006**, *312*, 885.
[11] H.-M. Xiong, Y. Xu, Q.-G. Ren, Y.-Y. Xia, *J. Am. Chem. Soc.* **2008**, *130*, 7522.
[12] F. Jiao, H. Frei, *Angew. Chem. Int. Ed.* **2009**, *48*, 1841.
[13] J.-H. Lee, Y.-M. Huh, Y.-w. Jun, J.-w. Seo, J.-t. Jang, H.-T. Song, S. Kim, E.-J. Cho, H.-G. Yoon, J.-S. Suh, J. Cheon, *Nat. Med.* **2007**, *13*, 95.
[14] H. J. Fan, M. Knez, R. Scholz, K. Nielsch, E. Pippel, D. Hesse, M. Zacharias, U. Gösele, *Nat. Mater.* **2006**, *5*, 627.
[15] M. T. Klem, D. A. Resnick, K. Gilmore, M. Young, Y. U. Idzerda, T. Douglas, *J. Am. Chem. Soc.* **2007**, *129*, 197.
[16] a) N. W. Ockwig, O. Delgado-Friedrichs, M. O'Keeffe, O. M. Yaghi, *Acc. Chem. Res.* **2005**, *38*, 176; b) S. Kitagawa, R. Kitaura, S.-i. Noro, *Angew. Chem. Int. Ed.* **2004**, *43*, 2334; c) M. Oh, G. B. Carpenter, D. A. Sweigart, *Acc. Chem. Res.* **2004**, *37*, 1.
[17] X. Sun, S. Dong, E. Wang, *J. Am. Chem. Soc.* **2005**, *127*, 13102.
[18] Z. Ni, R. I. Masel, *J. Am. Chem. Soc.* **2006**, *128*, 12394.
[19] a) S. Jung, W. Cho, H. J. Lee, M. Oh, *Angew. Chem. Int. Ed.* **2009**, *48*, 1459; b) X. Liu, *Angew. Chem. Int. Ed.* **2009**, *48*, 3018.
[20] W. Cho, H. J. Lee, M. Oh, *J. Am. Chem. Soc.* **2008**, *130*, 16943.
[21] G. A. Ozin, A. C. Arsenault, *Nanochemistry: A Chemical Approach to Nanomaterials* , RSC Publishing, Cambridge,UK **2005**.
[22] L. Guo, Y. L. Ji, H. Xu, P. Simon, Z. Wu, *J. Am. Chem. Soc.* **2002**, *124*, 14864.
[23] W. Cho, Y. H. Lee, H. J. Lee, M. Oh, *Chem. Commun.* **2009**, 4756.
[24] N_2 adsorption isotherm of **4a** exhibits the behavior for multilayer adsorption typical for nonporous or macroporous materials with a Brunauer-Emmett-Teller (BET) specific surface area (S_{BET}) of 8.8 $m^2 g^{-1}$ and a Langmuir surface area of 11.8 $m^2 g^{-1}$ (see Figure S14).
[25] a) A. D. Dinsmore, M. F. Hsu, M. G. Nikolaides, M. Marquez, A. R. Bausch, D. A. Weitz, *Science* **2002**, *298*, 1006; b) F. Caruso, *Chem. Eur. J.* **2000**, *6*, 413; c) J. Liu, D. Xue, *Adv. Mater.* **2008**, *20*, 2622; d) J. Shin, R. M. Anisur, M. K. Ko, G. H. Im, J. H. Lee, I. S. Lee, *Angew. Chem. Int. Ed.* **2009**, *48*, 321; e) Y. Piao, J. Kim, H. B. Na, D. Kim, J. S. Baek, M. K. Ko, J. H. Lee, M. Shokouhimehr, T. Hyeon, *Nat. Mater.* **2008**, *7*, 242.
[26] ICP analysis for the initial Zn-MSB-Zn (**2a**) and the cation exchanged products of Cu-MSB-Zn (**3a**) and Co-MSB-Zn (**3b**) shows the decrease in the Zn content (from 29.06 to 15.93 for **3a** and 17.62% for **3b**) and the increase in the Cu content (from 0 to 15.22%) for **3a** and the Co content (from 0 to 9.64%) for **3b**.
[27] The emission spectrum of Co-MSB-Zn (**3b**) is almost identical to that of Co-MSB-Co (**2b**); this is ascribed to the fact that their fluorescent properties originate from the constituent weakly fluorescent Co-MSB building blocks. See Figure S1 for the emission spectra of a series of CPPs.
[28] S.-F. Zheng, J.-S. Hu, L.-S. Zhong, W.-G. Song, L.-J. Wan, Y.-G. Guo, *Chem. Mater.* **2008**, *20*, 3617.
[29] Two metals were simultaneously discovered on certain area in elemental mapping images because two or more nanoparticles were stacked on certain area of ball's layer.
[30] ICP analysis of the initial Co-MSB-Co (**2b**) and the cation exchanged products of Cu-MSB-Co (**3c**) and Ni-MSB-Co (**3d**) confirms a decrease in the Co content (from 21.18 to 13.44 for **3c** and 11.98% for **3d**) and an increase in the Cu content (from 0 to 12.51%) for **3c** and the Ni content (from 0 to 9.93%) for **3d**.
[31] L. Li, L. Chen, R. Qihe, G. Li, *Appl. Phys. Lett.* **2006**, *89*, 134102.